Simulation of the Electric Field on High Voltage Insulators using the Finite Element Method

Vassiliki T. Kontargyri, Ioannis F. Gonos, *Member, IEEE*, Ioannis A. Stathopulos, and Alex M. Michaelides

***Abstract*—The paper presents a study into the potentials and electric field distribution on insulator strings, which are used for suspension of overhead transmission lines of 400kV and are stressed by power frequency voltage. The investigated insulator strings are used by the Public Power Corporation of Greece in high voltage transmission networks. The Finite Element Analysis (FEA) program OPERA was used to carry out the electric field analysis on the insulators. Two types of insulator strings were investigated, the first using porcelain and the second using glass as the insulating material. A comparative analysis of these insulators is presented.**

***Index Terms*—Insulators, electric fields, simulation software, finite element methods.**

I. Introduction

The insulators, which are used for the suspension of overhead transmission lines, constitute one of the most important parts of the transmission lines as flashover effects in insulators can cause the breakdown of a transmission network. The electric field distribution within and around high voltage insulators is a very important aspect of the design of the insulators. Also the knowledge of the electric field could be useful for the detection of defects in insulators [1].

Several methods have been developed for the computation of electric fields and potentials along an insulator string [2-4]. In this paper, the electric field and potential distribution around and inside the insulator when it is stressed by power frequency voltage is examined using OPERA, which is a suite of programs for two and three dimensional electromagnetic field ana1ysis [5, 6]. The software package uses the finite element method to solve the partia1 differential equations that describe the behaviour of electromagnetic fields. The results of the two and three dimensional simulation models are compared and the critical points affecting simulation accuracy are examined. The use of alternative formulations for improvement of results is also proposed.

Manuscript received April 24, 2006. This work is co - funded by the European Social Fund (75%) and National Resources (25%) - Operational Program for Educational and Vocational Training II (EPEAEK II) and particularly by the Program HERAKLEITOS.

V. T. Kontargyri, I. F. Gonos, I. A. Stathopulos are with the School of Electrical and Computer Engineering, National Technical University of Athens, 157 80 GREECE (phone: +30-210-7722226, +30-210-7723582; fax: +30-210-7723504; e-mails: vkont@central.ntua.gr, igonos@ieee.org, stathop@ power.ece.ntua.gr).

A. M. Michaelides is with the Vector Fields, U.K., 24 Bankside, Kidlington, Oxford OX5 1JE, U.K. (e-mail: Alex.Michaelides@vectorfields.co.uk).

II. Electric Field and Potential Formulation

The electric field intensity E is given by [4]:

$$\mathbf{E} = -\nabla V \quad (1)$$

The divergence of the electric flux density **D** is related to the charge density ρ:

$$\nabla \mathbf{D} = \rho \quad (2)$$

Combining equations (1) and (2) and introducing the dielectric permittivity tensor ε ($\mathbf{D} = \varepsilon \mathbf{E}$) arises the usual Poisson's equation description of the electrostatic potential:

$$\nabla \cdot \varepsilon \nabla V = -\rho \quad (3)$$

A similar equation arises for current flow problems,

$$\nabla \cdot \sigma \nabla V = 0 \quad (4)$$

where σ is the conductivity, and $\mathbf{J} = \sigma \mathbf{E}$.

III. Investigated Insulators

The examined cap-and-pin type insulators are used for the suspension of 400kV overhead transmission lines. Each insulator string consists of 18 disc insulators. At one edge of the insulator string (18th insulator) is connected a transmission line and the other edge (1st insulator) is grounded. The geometrical characteristics of the porcelain insulator are the diameter (*d*), which is 320mm, the height (*h*), which is 170mm, and the creepage distance (*L*), which is 540mm. The corresponding characteristics of the glass insulator are *d*=280mm, *h*=150mm and *L*=370mm. It is observed that the creapage distance of the porcelain insulator is longer than the creapage distance of the glass insulator, therefore the porcelain insulator is characterized as fog type and is used in areas with high humidity and pollution.

IV. Results and Discussion

The paper discusses the application of two and three dimensional FEA for the modeling of the insulators, as well as the solution formulations appropriate for this class of problem.

The glass insulator string has been simulated in Opera-2d. In order to design the model of the insulator string in the two dimensional program the axi-symmetry of the problem is exploited. Figs. 1 and 2 illustrate the potential and the electric field, respectively, inside and around the 17th and the 18th insulator which are nearer the transmission line and therefore are more highly stressed.

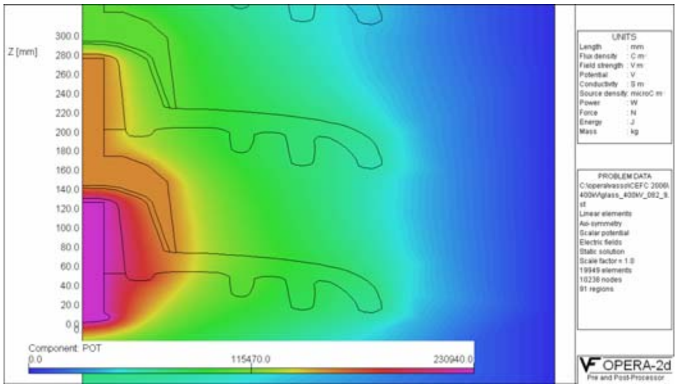

Fig. 1. Potential contours of a part of the glass insulator string.

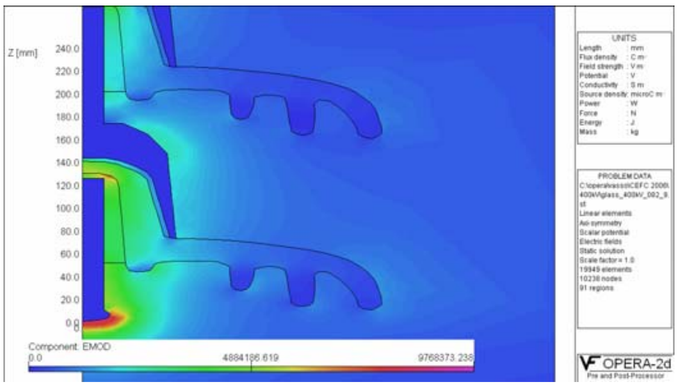

Fig. 2. Electric field contours of a part of the glass insulator string.

The axi-symmetry of the problem is destroyed by the existence of excited and ground conductors which must be included in the three-dimensional model to correctly represent the device. Hence, the cap-and-pin insulator string structures were also simulated using OPERA-3d. In these models, a section of the transmission line is also included. The length of the conductor included in the model was set to be approximately equal with the length of the insulator string [4]. Further increase in the length of the conductor would result in negligible improvement to the accuracy of the results, while unnecessarily increasing computation times.

Fig. 3 presents the three dimensional model of the glass insulator string. The conductor is parallel to the X-axis and the insulator string is parallel to the Z-axis.

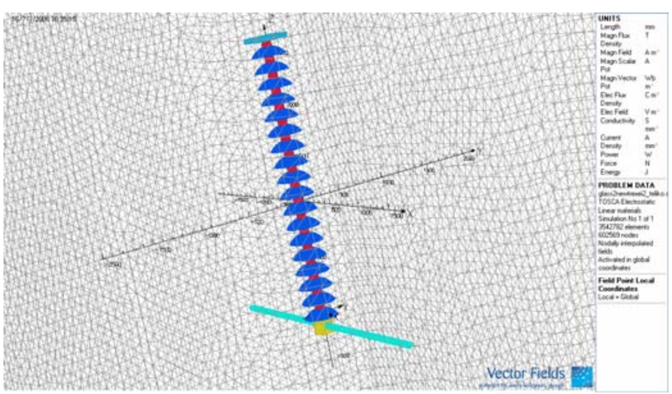

Fig. 3. The three dimensional model of the glass insulator string.

Fig. 4 illustrates the potential distribution on a cartesian patch on a YZ plane for the cap-and-pin glass insulator string structure. The part of the insulator string nearer the conductor is more highly stressed.

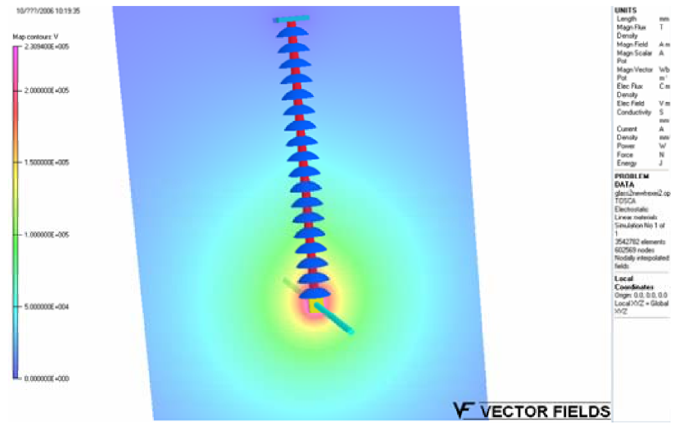

Fig. 4. Potential distribution of the glass insulator string.

Fig. 5 presents the electric field as a histogram on a cartesian patch on the YZ plane through the center of the glass insulator string.

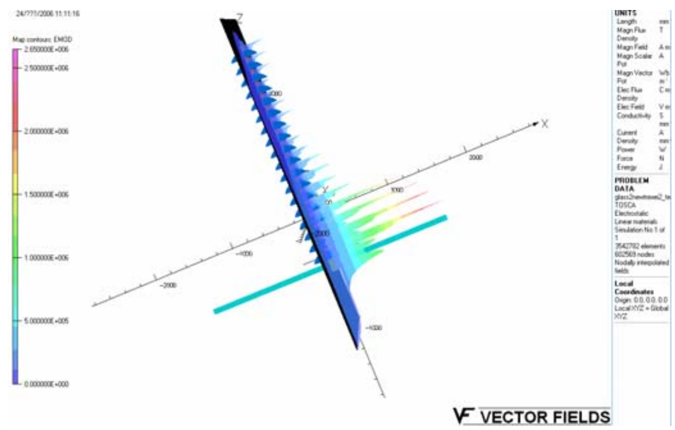

Fig. 5. Histogram of the electric field in a cartesian patch on YZ plane of the glass insulator string.

Figs. 6 and 7 represent the potential and the electric field distribution, respectively, along a set of lines running parallel to the axis of the insulators (Z-axis) and at different distances from it. The above lines are vertical to the conductor (X-axis). The continuous line in the graph of the potential passes through the axis of the insulator string. The step-variation of the potential is due to the presence of the conducting parts of the insulator string.

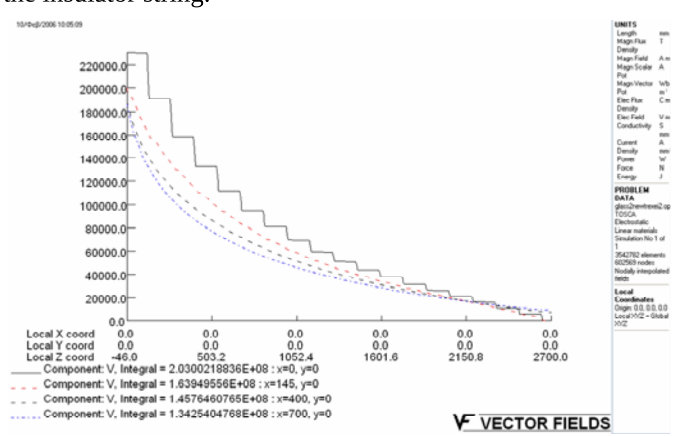

Fig. 6. Potential along lines parallel to the glass insulator string and vertical to the conductor (X-axis).

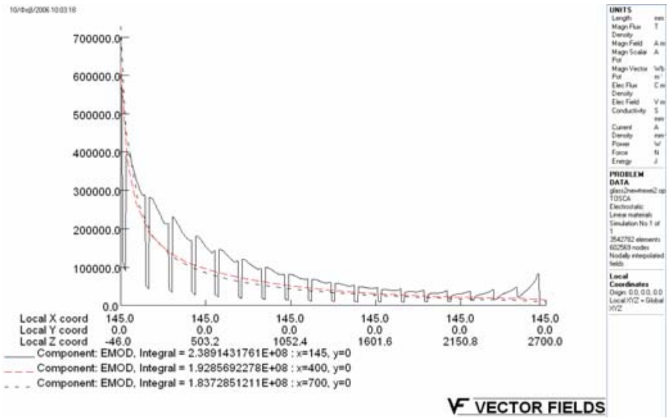

Fig. 7. Electric field along lines parallel to the glass insulator string and vertical to the conductor (X-axis).

Figs. 8 and 9 illustrate the potential and the electric field distribution, respectively, along a set of lines running parallel to the Z-axis and perpendicular to the Y-axis (away from the conductor). Comparing the values of the potential and the electric field that have been arisen from Figs. 6 and 7 with the respective values of Figs. 8 and 9, the potential and the electric field levels of Figs. 6 and 7 are higher as the lines are sited nearer the excited conductor. This variation in the field can not be accounted for in the two dimensional model and hence the necessity for three dimensional simulations.

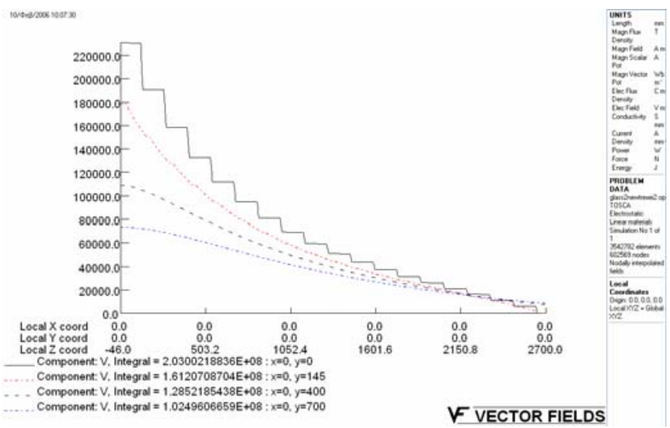

Fig. 8. Potential along lines parallel to the glass insulator string and vertical to the Y-axis.

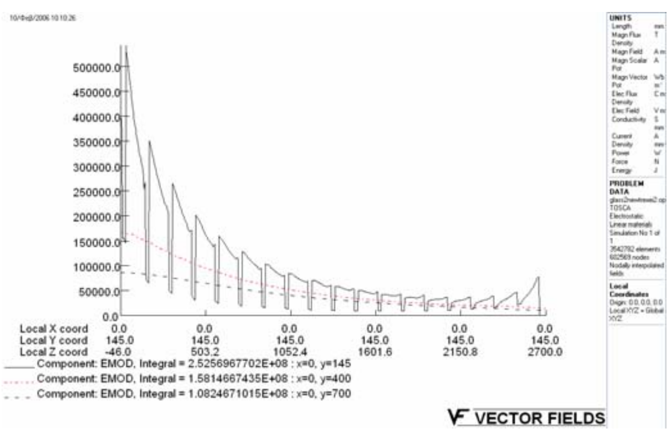

Fig. 9. Electric field along lines parallel to the glass insulator string and vertical to the Y-axis.

In addition, a porcelain cap-and-pin insulator string structure, which is used for the suspension of 400kV overhead transmission lines, was also simulated using OPERA-3d. In Fig. 10 the geometry of the model and the histogram of the potential on a cartesian patch on the YZ plane passing through the center of the insulator string are shown.

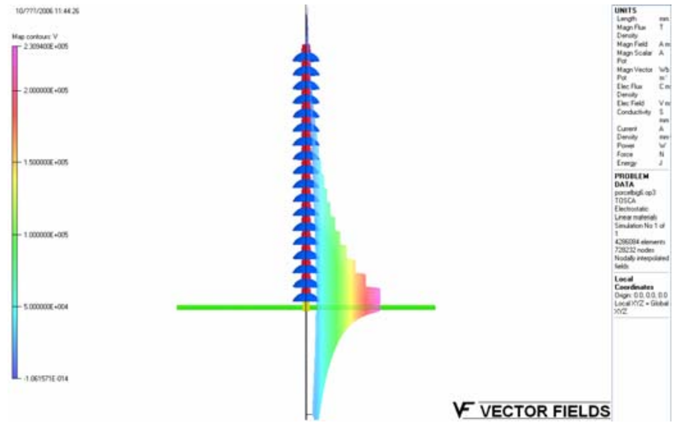

Fig. 10. Histogram of the potential in a cartesian patch on YZ plane of the porcelain insulator string.

Fig. 11 presents the potential distribution along a set of lines running parallel to the axis of the insulators (Z-axis) and at different distances from this. The above lines are perpendicular to the conductor (X-axis).

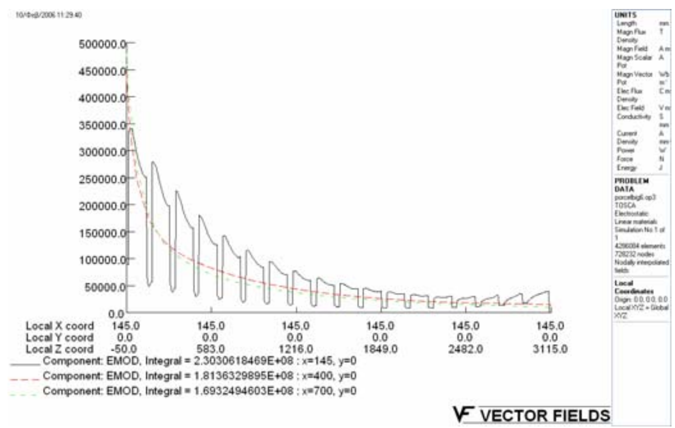

Fig. 11. Electric field along lines parallel to the porcelain insulator string and vertical in the X-axis.

Figs. 12 and 13 show one comparison of the potential and the electric field distribution along a line running vertically through the edges of the insulators of the porcelain and the glass insulator string.

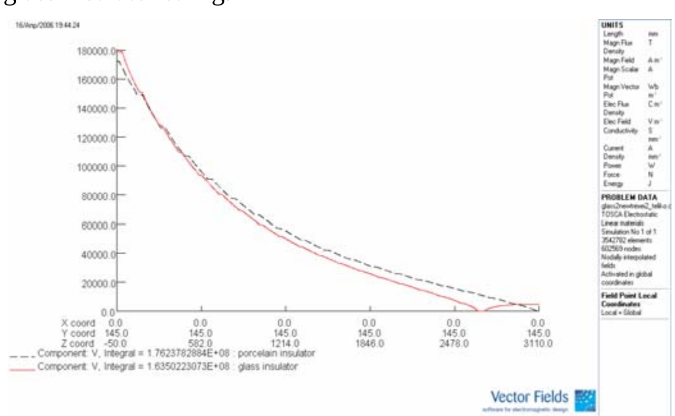

Fig. 12. Potential along porcelain and glass insulator string.

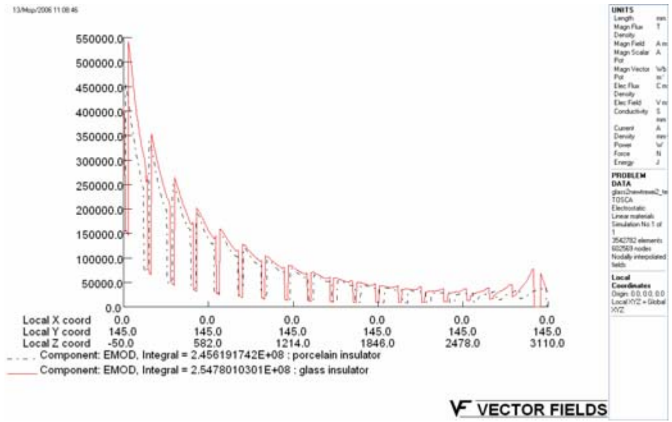

Fig. 13. Electric field along porcelain and glass insulator string.

The electric field levels recorded in the glass insulator string are higher than those of the porcelain insulator. The dielectric characteristics of the porcelain are such that this type of insulator string offers a smoother distribution of the electric field along it. The higher electric field levels recorded in the glass insulator are, however, still sustainable owing to the higher dielectric strength of the glass.

Finally, a comparison between results from two and three dimensional analysis of the glass insulator string is presented in Fig. 14. The percentage of the voltage, which is applied in the i-insulator of the insulator string, is compared for the two models. Owing to parasitic capacitances, the distribution of the voltage in each insulator is not uniform. The slope of the curve arising from OPERA-3d is lower than that of the curve arising from OPERA-2d results. In addition, the shape of the curve obtained in OPERA-3d is in agreement with experimental results for high voltage ceramic insulator strings [7].

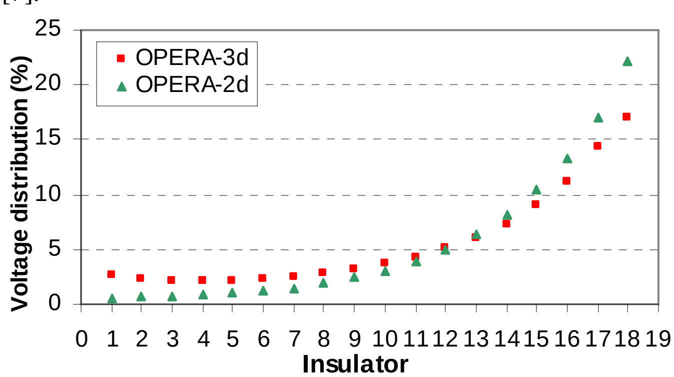

Fig. 14. Comparison between two and three dimensional models of the glass insulator string.

For this class of problems, the electrostatic solution presents the limitation that the materials are characterized only by their dielectric properties. In order to construct a model that provides more accurate results, the conducting and dielectric properties of the materials must both be accounted for. The application of alternative formulations that account for the conducting and dielectric properties of the materials in a three-dimensional simulation is a point for future research. In its simplest form, a combined solution would involve an initial solution of the current flow problem, the output of which is used as a boundary condition for the electrostatic problem [8].

In time-varying problems, the electric and magnetic fields are normally solved in a coupled manner. Assuming that inductive effects are negligible in semi-conducting dielectric problems, the program would solve for [8]

$$\nabla \cdot \varepsilon_c \, \nabla V = 0$$

where,

$$\varepsilon_c = \varepsilon_0 \varepsilon_r - j\frac{\sigma}{\omega}$$

Results from OPERA-2d simulations have demonstrated the benefits of such formulations and the adoption of these in the three-dimensional modeling of insulators is currently underway.

V. Conclusions and Future Work

A method for the calculation of the potential and the electric field, which is proposed in this paper, is applicable in every type of insulator. The simulation models of the insulator structures are a useful tool for the designers of the transmission network. The correct design of the insulator and the determination of the correct material properties are paramount in the goal to achieve accurate simulation results. It has been demonstrated that, although the device is primarily axi-symmetric, a complete three-dimensional solution offers significant insight into the detailed field distribution. Results from OPERA-2d lossy-dielectric solutions of insulators [7, 8], have also demonstrated the benefits of such analysis. The next goal would now be to complete the loop, by including a combination of the dielectric constant and the conductivity of the materials in a three-dimensional simulation.

References

[1] Power Systems Research Center, *Evaluation of Critical Components of Non-Ceramic Insulators (NCI) In-Service: Role of Defective Interfaces,* Final Project Report, PSERC Publications 04-32, Arizona, August 2004.

[2] J. L. Rasolonjanahary, L. Krähenbühl, and A. Nicolas, “Computation of electric fields and potential on polluted insulators using a boundary element method”, *IEEE Transactions on Magnetics*, Vol. 38, No. 2, pp. 1473-1476, March 1992.

[3] I. Sebestyén, “Electric-field calculation for HV insulators using domain-decomposition method”, *IEEE Transactions on Magnetics*, Vol. 38, No. 2, pp. 1213-1216, March 2002.

[4] T. Zhao, M. G. Comber, “Calculation of Electric Field and Potential Distribution Along Nonceramic Insulators Considering the Effects of Conductors and Transmission Towers”, *IEEE Transactions on Power Delivery*, Vol. 15, No. 1, pp. 313-318, January 2000.

[5] Vector Fields, *OPERA-2d Reference Manual*, Vector Fields Limited, England, November 2004.

[6] Vector Fields, *OPERA-3d Reference Manual*, Vector Fields Limited, England, November 2004.

[7] V. T. Kontargyri, I. F. Gonos, I. A. Stathopulos, A.M. Michaelides, “Calculation of the electric field on an insulator using the Finite Elements Method”, *Proceedings of the 38th International Universities Power Engineering Conference (UPEC 2003)*, Thessaloniki, Greece, September 1-3, 2003, pp. 65-68.

[8] A. M. Michaelides, C. P.. Riley, A. P. Jay, G. Molinari, P. Alotto, A. Zubiani, A. D’Souza and J. Madail Vaiga, “Parametric FEA for the Design of electric insulating components”, *Proceedings of the 3rd Mediterranean Conference on Power Generation, Transmission and Distribution and Energy Conversion (MEDPOWER 2002)*, Athens, Greece, November 4-6, 2002.